DALTON
FULL PAPER

Self-assembling iron and manganese metal–germanium–selenide frameworks: $[NMe_4]_2MGe_4Se_{10}$, where M = Fe or Mn

Homayoun Ahari, Armando Garcia, Scott Kirkby, Geoffrey A. Ozin,* David Young and Alan J. Lough

Materials Chemistry Research Group, Lash Miller Chemical Laboratories, University of Toronto, 80 St. George Street, Toronto, Ontario, Canada M5S 3H6

The hydrothermal synthesis mixture Ge–Se–(TMA)OH–H_2O ($TMA^+ = NMe_4^+$) yielded crystals of the material $(TMA)_4Ge_4Se_{10}$. A single-crystal X-ray diffraction structure showed the presence of adamantanoid $Ge_4Se_{10}^{4-}$ clusters and TMA^+ cations. The TMA^+ template-mediated aqueous synthesis of $(TMA)_2MGe_4Se_{10}$ (M = Mn or Fe) from $Ge_4Se_{10}^{4-}$ and M^{2+} building-blocks is described. Rietveld powder X-ray diffraction full profile structure refinements of $(TMA)_2MGe_4Se_{10}$ established that these novel metal–germanium–selenide frameworks are isostructural with the analogous metal–germanium–sulfides, $(TMA)_2MGe_4S_{10}$. The selenide materials have a zinc blende-type of open-framework structure. Charge-balance of the anionic open-framework $[MGe_4Se_{10}]^{2-}$ is maintained by two TMA^+ template cations that reside within the cavity spaces. Trends in the tetragonal unit cell dimensions and metal–chalcogenide bond lengths of $(TMA)_2MGe_4X_{10}$ (X = S or Se) are those expected based upon increases in metal and chalcogenide radii on passing from S^{-II} to Se^{-II} and Fe^{II} to Mn^{II}.

Controlled compositional variations of solid-state inorganic materials using isomorphous substitution, doping and defect chemistry is the foundation of tailoring their synthesis, structure, property and function relations.[1] Nowhere is this more apparent than in silicon, gallium arsenide and zinc sulfide semiconductor materials and devices, where their properties are controlled through compositional tuning between isostructural end-members, exemplified by Si/Ge, GaAs/AlAs and ZnS/ZnSe. Thus, Si_xGe_{1-x} alloys are used in high mobility transistors, $Al_xGa_{1-x}As$ to engineer the electronic band structure of quantum devices, $Ga_{1+x}As/GaAs_{1+x}$ to control the number of charge carriers in pn-doped laser diodes, ZnS_xSe_{1-x} to tailor the absorption properties of IR detectors and the emission characteristics of blue-green laser diodes.[2] These devices function on the principle of a random distribution of the elemental constituents over the tetrahedral sites of close-packed diamond- and zinc blende-types of crystal lattices.

Recently, we applied this paradigm to isostructural tin(IV) thioselenide open-framework materials.[3] The end-members have a framework that is based upon 2-D parallel-stacked microporous anionic $[Sn_3X_7]^{2-}$ layers, where X = S or Se. The individual layer topology is a 24-atom-ring hexagonal net. The pores are made up of broken cube Sn_3X_4 clusters connected *via* $Sn(\mu\text{-}X)_2Sn$ bridges. The tetramethylammonium (TMA^+) charge balancing cations are positioned within the pores and between the layers. In the ternary $(TMA)_2Sn_3S_xSe_{7-x}$ materials where $0 \leqslant x \leqslant 7$, it was established that the distribution of the chalcogenides is random (solid–solution, Vegard law) at the length scale of the unit cell but site-selective at the level of the trigonal bipyramidal building blocks.[4]

In a related system, the self-assembly of $Ge_4S_{10}^{4-}$ and M^{2+} building blocks, mediated by the TMA^+ template, produces an isostructural family of $(TMA)_2MGe_4S_{10}$ materials (where M = Mn, Fe, Co or Zn).[5–8] Their structure is based upon a zinc blende-type open framework with the tetragonal space group $I\bar{4}$ and unit cell dimensions in the range $a = 9.400$–9.513 and $c = 14.026$–14.281 Å. The tetrahedral sites in the lattice are alternately substituted by pseudo-tetrahedral M^{2+} and adamantanoid $Ge_4S_{10}^{4-}$ building blocks, all covalently linked together by M(μ-S)Ge bridge bonds. Charge balance of the anionic framework $[MGe_4S_{10}]^{2-}$ is maintained by two TMA^+ template cations that reside within the cavity spaces.

The isostructurality of the family of zinc blende-type open-frameworks $(TMA)_2MGe_4S_{10}$ provides an excellent opportunity for compositional tuning of their properties *via* the synthesis of $(TMA)_2M_xM'_{1-x}Ge_4S_{10}$ solid solutions, where $0 \leqslant x \leqslant 1$.[6] The distribution of the M^{2+}/M'^{2+} cations over the pseudo-tetrahedral sites that link together the $Ge_4S_{10}^{4-}$ adamantanoid modules controls the properties of these materials. Another approach for property tailoring in this system involves crystallizing mixtures of the precursors M^{2+}, $xGe_4S_{10}^{4-}$ and $(1-x)Ge_4Se_{10}^{4-}$ to give $(TMA)_2M(Ge_4S_{10})_x(Ge_4Se_{10})_{1-x}$, where $0 \leqslant x \leqslant 1$.

As a step in this direction we report the synthesis and single-crystal X-ray diffraction (XRD) structure determination of the adamantanoid $(TMA)_4Ge_4Se_{10}$ precursor as well as Rietveld powder X-ray diffraction (PXRD) full profile structure refinements of $(TMA)_2MGe_4Se_{10}$, where M = Mn or Fe, which establishes that these metal–germanium–selenide frameworks are isostructural with the analogous metal–germanium–sulfides, $(TMA)_2MGe_4S_{10}$.[5–8]

Experimental

Synthesis

A note of safety. All the synthetic procedures outlined in this paper must be carried out in a fumehood. A self-contained aspirator pump is essential for this type of work in order to prevent discharge of volatile amines and alkyl selenides from the filtrate.

$(TMA)_4Ge_4Se_{10}$. Yellow cube-shaped crystals were obtained from the hydrothermal synthesis system with a reaction ratio of $4.1(TMA)OH{\cdot}5H_2O : 4Ge : 10Se : 130H_2O$. A reaction mixture, consisting of 2.28 g $(TMA)OH{\cdot}5H_2O$, 4.4 g H_2O, 2.43 g Se and 0.89 g Ge, following the same order of addition, was placed into a Teflon™-lined stainless steel reactor and heated hydrothermally at 150 °C for 3 d in a rolling oven. The product was recovered using suction filtration. The mass yield was 1.39 g which corresponded to a yield of 33% assuming no hydration in the final dry product.

$(TMA)_2MGe_4Se_{10}$ (M = Mn or Fe). These compounds can

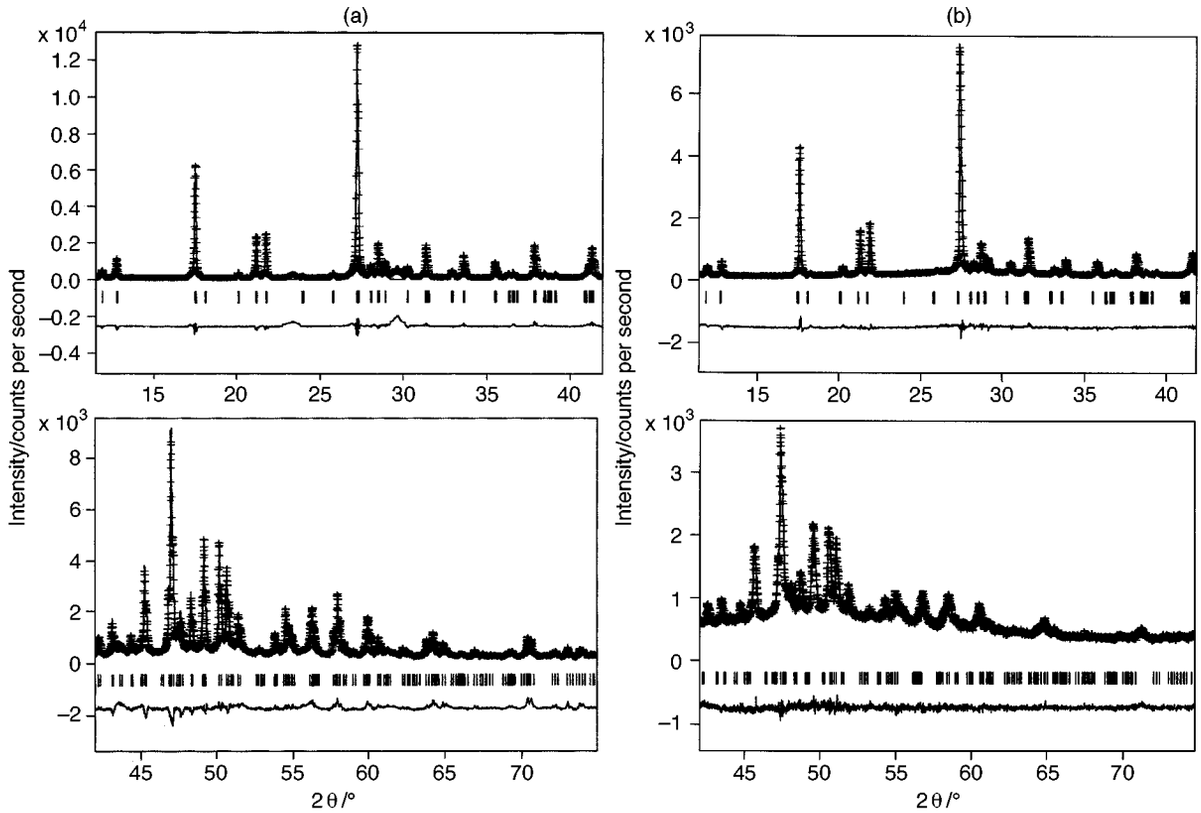

Fig. 1 Observed (+, I_o), calculated (--, I_c) and difference ($I_o - I_c$) high resolution room-temperature PXRD patterns of (a) $(TMA)_2MnGe_4Se_{10}$ and (b) $(TMA)_2FeGe_4Se_{10}$

be synthesized and crystallized from water by simply mixing together aqueous solutions of the M^{2+} and adamantanoid $Ge_4Se_{10}^{4-}$ building-blocks. Control over the rates of nucleation and crystal growth has been achieved through reaction profiles that examine the effects of temperature, selective complexation, mineralization and transporting agents and diffusion crystal growth. Optimization of the product yield, phase purity and degree of crystallinity (PXRD) of $(TMA)_2MGe_4Se_{10}$ was achieved in syntheses that employed the following reaction stoichiometries and weights of reagents: $(TMA)_4Ge_4Se_{10}$ (0.35 g, 0.25 mmol), $FeSO_4{\cdot}7H_2O$ (0.078 g, 0.28 mmol), H_2O (9.15 g, 510 mmol) giving a yield of 0.20 g for $(TMA)_2FeGe_4Se_{10}$; and $(TMA)_4Ge_4Se_{10}$ (0.35 g, 0.25 mmol), $Mn(OAc)_2{\cdot}4H_2O$ (0.069 g, 0.28 mmol), H_2O (9.15 g, 510 mmol) giving a yield of 0.18 g for $(TMA)_2MnGe_4Se_{10}$. The products $(TMA)_2MGe_4Se_{10}$ are essentially phase pure (aside from a trace of poorly crystalline selenium formed on storage of the materials in air at room temperature; they appear indefinitely stable when stored below 0 °C under an Ar atmosphere). The $(TMA)_2MGe_4Se_{10}$ products are orange (Mn) and red (Fe) in color. The crystal morphology is best described as a tetragonal tetrahedron or tetragonal disphenoid, which is characterized by four isosceles triangular faces with the four-fold improper rotation axis bisecting two opposite edges. The crystals varied in size between 1 and 20 microns.

Powder X-ray diffraction and Rietveld structure refinement

Room-temperature X-ray powder diffraction data of $(TMA)_2MGe_4Se_{10}$ were collected on a Siemens D-5000 diffractometer (Fig. 1) using a Cu tube source and a 'drifted Li–Si' solid-state detector whose energy window was centered at 8.04 keV ($eV \approx 1.602 \times 10^{-19}$ J). The detector was set to discriminate against Cu-Kβ, leaving the Cu-K$\alpha_{1,2}$ X-ray lines. Voltage and current settings of the X-ray tube were 50 kV and 35 mA, respectively. The samples were packed onto low background flat plates. For practical reasons the data were collected in two sections from 10 to 42° and from 42 to 75° 2θ. This allowed the collection of high signal-to-noise data in the upper range while still keeping total collection times within acceptable limits for the X-ray facility. The Rietveld refinements were carried out using the General Structure Analysis System (GSAS).[9] The two ranges of each data set were fitted as two histograms for a single structural model. The unit cell starting values were obtained from indexing the lower range histogram. The single-crystal data for $(TMA)_2MnGe_4S_{10}$ were used to provide the initial atom positions within the unit cell and the $I\bar{4}$ space group. The atom positions were translated within the unit cell to place a $Ge_4Se_{10}^{4-}$ unit at the body center, rather than TMA^+. This was done for convenience during the refinement. The histograms were fitted by first refining the lattice parameters and the background function. Next the atom positions were allowed to vary, followed by the peak profile coefficients. The peaks were modeled as pseudo-Voigt functions. The starting values for the coefficients were determined by refining LaB_6, a line-shape standard [National Institute of Standards and Technology instrument line position and profile shape (SRM 660) LaB_6 diffraction standards]. Isotropic thermal parameters were constrained to positive values. Any factor that ran negative was replaced with GSAS's default value of 0.0250 and fixed before final refinement. The TMA^+ cations present in the void spaces of the framework were fitted as 'NC_4 rigid bodies' which maintained their structure. No attempt was made to fit the TMA^+ cations with the hydrogen atoms attached since past experience with room-temperature data Rietveld refinements has demonstrated no improved correlation of the results to those obtained by single-crystal diffraction methods. Efforts to fit the TMA^+ as independent atoms resulted in the failure of the refinement to converge to a sensible structure. This resulted from slight background electron density within the cavity. The most reasonable explanation is delocalization (likely thermal motion) of the TMA^+ cations about the special positions on which they are centered. All the refinements gave R_p values of less than 9% indicating acceptable fits.

Table 1 Pertinent crystallographic information for $(TMA)_2MGe_4X_{10}$, where M = Mn or Fe; X = S or Se

	Tetragonal $I\bar{4}$			
Parameter	$(TMA)_2MnGe_4S_{10}$[5–8]	$(TMA)_2FeGe_4S_{10}$[8]	$(TMA)_2MnGe_4Se_{10}$	$(TMA)_2FeGe_4Se_{10}$
a/Å	9.513(1)	9.429(4)	9.767(4)	9.696(5)
c/Å	14.281(2)	14.206(6)	14.833(6)	14.705(8)
U/Å^3	1292.4	1263.0	1415.0	1382.5
$r(GeX_t)$/Å	2.159	2.132	2.289	2.241
$r(GeX_b)$*/Å	2.243–2.218	2.259–2.107	2.380–2.304	2.401–2.317
$r(MX_t)$*/Å	2.440	2.298	2.552	2.502
$\alpha(X_tMX_t)$/°	124.5	119.0	127.5	125.5
$\beta(X_tMX_t)$/°	102.5	104.9	101.3	102.1

* Range of three distinct germanium–chalcogenide Ge_4X_{10} intracluster bond lengths.

Table 2 Fractional atomic parameters for $(TMA)_2MnGe_4Se_{10}$[a]

Atom[b]	x	y	z	U(iso)/Å^2
Ge(1)	0.078 9(4)	0.176 3(4)	0.088 5(3)	0.0250
Se(2)	0.260 4(4)	0.103 1(3)	−0.006 7(3)	0.0250
Se(3)	0.000 0	0.000 0	0.186 3(3)	0.0250
Se(4)	0.176 3(4)	0.345 5(4)	0.173 9(3)	0.0250
N(1)	0.500 0	0.500 0	0.000 0	0.0250
C(1)	0.374 680	0.466 050	−0.062 040	0.06(1)
N(2)	0.500 0	0.000 0	0.250 0	0.0250
C(2)	0.422 350	−0.101 640	0.189 890	0.0250
Mn(1)	0.000 0	0.500 0	0.250 0	0.0250

[a] Rietveld refinement statistics for $(TMA)_2MnGe_4Se_{10}$; histogram 1: $Rw_p = 11.78\%$; $R_p = 8.72\%$; histogram 2: $Rw_p = 11.62\%$, $R_p = 9.08\%$; powder totals: $Rw_p = 11.67\%$, $R_p = 8.98\%$; $\chi_R^2 = 6.902$. [b] The high precision for the carbon atom positions is the product of the rigid body refinement of the TMAs with the nitrogen atoms in the special positions.

Table 3 Fractional atomic parameters for $(TMA)_2FeGe_4Se_{10}$[a]

Atom[b]	x	y	z	U(iso)/Å^2
Ge(1)	0.078 9(5)	0.181 1(5)	0.089 2(4)	0.047(3)
Se(1)	0.263 7(5)	0.106 5(4)	−0.006 0(4)	0.041(3)
Se(2)	0.000 0	0.000 0	0.187 7(5)	0.040(3)
Se(3)	0.173 8(5)	0.350 2(4)	0.172 2(3)	0.027(2)
N(1)	0.500 0	0.500 0	0.000 0	0.40(8)[c]
C(1)	0.374 680	0.466 050	−0.062 040	0.0250
N(2)	0.500 0	0.000 0	0.250 0	0.0250
C(2)	0.422 350	−0.101 640	0.189 890	0.33(6)[c]
Fe(1)	0.000 0	0.500 0	0.250 0	0.086(7)

[a] Rietveld refinement statistics for $(TMA)_2FeGe_4Se_{10}$; histogram 1: $Rw_p = 10.83\%$; $R_p = 8.04\%$; histogram 2: $Rw_p = 4.96\%$, $R_p = 3.90\%$; powder totals: $Rw_p = 7.22\%$, $R_p = 5.13\%$; $\chi_R^2 = 2.614$. [b] The high precision for the carbon atom positions is the product of the rigid body refinement of the TMAs with the nitrogen atoms in the special positions. The large thermal parameters on the atoms of TMA^+ cations may be due to some disorder of these molecules. Attempts to model these molecules as disordered atoms gave no improvement in the structure refinement and in fact the model using the anisotropic thermal displacement parameters gave the better results. [c] The void space in which the TMA^+ sits is larger than the close-packing space of the molecules. It is therefore expected to rattle around in the cavity space at room temperature among four lowest energy sites given the S_4 symmetry. However, the space group and coordinate system chosen puts the N on a special position where it cannot move. The result would be a large C–N displacement vector and a large thermal parameter for N which is what is found. When it is attempted to fit the system with the N off the special position and using a complete TMA^+ cation, the fit was not any better and there were so many new TMA^+ parameters from all the symmetry requirements that it did not provide any more meaning and might just be mopping up errors.

As expected the Rietveld refinements confirmed that $(TMA)_2MGe_4X_{10}$ (M = Mn^{2+} or Fe^{2+}; X = S or Se) are all isostructural, but with variations in the unit-cell parameters and in some of the atom positions within the unit cell (see Table 1). Unit-cell parameters, atom positions and Rietveld refinement statistics are listed in Tables 2 and 3.

CCDC reference number 186/979.

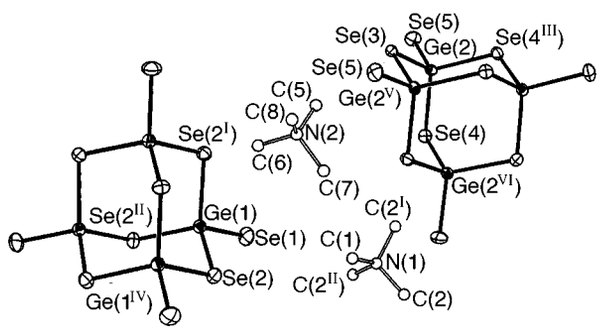

Fig. 2 An ORTEP diagram of single-crystal XRD structure of $(TMA)_4Ge_4Se_{10}$, H atoms are omitted for clarity

Results and Discussion

The compound $(TMA)_4Ge_4Se_{10}$ crystallizes in the cubic space group $P\bar{4}3n$ with $a = 20.028(2)$ Å. There are eight $Ge_4Se_{10}^{4-}$ clusters in the cubic unit cell with two crystallographically distinct sites. Two of these units are located on the mid line of each face for a total of six, while the others lie at the center and corners accounting for the remaining two. Fig. 2 shows a labeled thermal ellipsoid drawing (ORTEP)[10] of the molecule. There are also two crystallographically distinct sites for the charge balancing TMA^+ cations in the unit cell. They form Ge–$Se_t\cdots$H–C (3.053, 3.112 Å) and Ge–$Se_b\cdots$H–C (3.028, 3.143 Å) hydrogen bonds involving methyl group hydrogen atoms of the TMA^+ cations and terminal and bridging selenium atoms of the adamantanoid $Ge_4Se_{10}^{4-}$ cluster. The purity of the as-synthesized $(TMA)_4Ge_4Se_{10}$ material was determined by the comparison of the X-ray powder pattern of the material with the simulated pattern created by CERIUS® software as shown in Fig. 3.[11] Details of the structure and summary of data collection for $(TMA)_4Ge_4Se_{10}$ are presented in Tables 4 and 5. The crystallographic information for $(TMA)_4Ge_4X_{10}$, where X = S or Se, is compared in Table 6.

The powder patterns of $(TMA)_2MGe_4Se_{10}$ (M = Mn or Fe) have been recorded under high resolution conditions on a Siemens D5000 diffractometer. They both indexed quite well in the tetragonal space group $I\bar{4}$ and yielded unit cell dimensions of $a = 9.767(4)$, $c = 14.833(6)$ Å (Mn) and $a = 9.696(5)$, $c = 14.705(8)$ Å (Fe). This provides evidence for isostructurality between all members of the family of materials, $(TMA)_2MGe_4X_{10}$, where M = Mn or Fe; X = S or Se, Table 1. The structure of $(TMA)_2MGe_4S_{10}$ has been determined from single-crystal XRD (M = Mn),[5] by *ab initio* structure determination[7] and Rietveld PXRD full profile (M = Fe, Co, Zn) structure analyses.[14] The phase has an open-framework structure based on the alternation, in all three spatial dimensions, of pseudo-tetrahedral M^{2+} and adamantanoid $Ge_4S_{10}^{4-}$ building-blocks, all covalently linked together by M(μ-S)Ge bridge-bonds and packed into a tetragonal $I\bar{4}$ unit cell with dimensions $a = 9.513(1)$, $c = 14.281(2)$ Å (Mn)[5–7] and $a = 9.429(4)$, $c =$

Table 4 Single-crystal XRD data and structure refinement for $(TMA)_4Ge_4Se_{10}$*

Empirical formula	$C_{16}H_{48}Ge_4N_4Se_{10}$
M	1376.54
T/K	168(2)
λ/Å	0.710 73
Crystal system	Cubic
Space group	$P\bar{4}3n$
a/Å	20.028(2)
U/Å^3, Z	8033.3(13), 8
D_c/Mg m^{-3}	2.276
μ/mm^{-1}	12.041
F(000)	5120
Crystal size/mm	0.31 × 0.29 × 0.27
θ Range/°	2.88 to 24.97
Limiting indices	$2 \leqslant h \leqslant 23$, $0 \leqslant k \leqslant 16$, $0 \leqslant l \leqslant 16$
Reflections collected	2492
Independent reflections	1297 (R_{int} = 0.0849)
Absorption correction	0.3547, 0.4274
Data, restraints, parameters	1297, 0, 81
Goodness of fit on F^2	0.708
Final R indices [$I > 2\sigma(I)$]: $R1$, $wR2$	0.0345, 0.0301
R indices (all data): $R1$, $wR2$	0.1333, 0.0394
Absolute structure parameter	0.34(8)
Extinction coefficient	0.000 060(2)
Largest difference peak, hole/e Å^{-3}	0.529, −0.552

* Mo-Kα radiation, graphite-monochromator, Enraf-Nonius CAD4 diffractometer, absorption correction (SHELXA-90 program for absorption correction),[12] structure solved by direct methods and refined by full-matrix least-squares on F^2 using SHELXTL/PC.[13] The Ge and Se atoms were refined with anisotropic displacement parameters and C and N atoms were refined isotropically. Hydrogen atoms were included in calculated positions and treated as riding atoms.

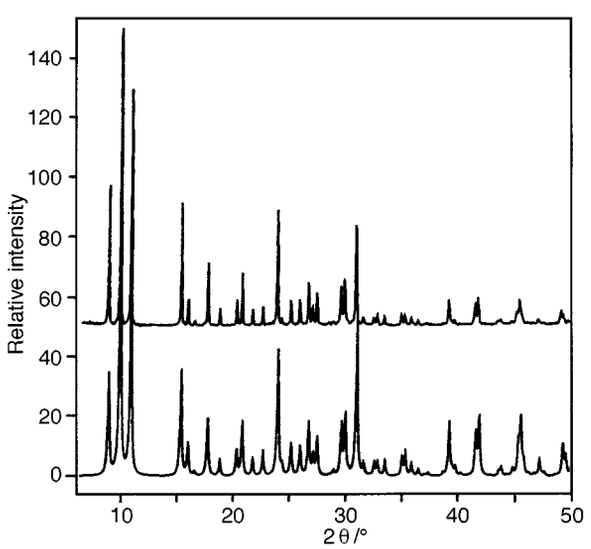

Fig. 3 X-Ray powder pattern for $(TMA)_4Ge_4Se_{10}$ (top) compared with the simulated powder pattern (bottom) from single-crystal data, created by CERIUS® software

14.206(6) Å (Fe).[8] With these structures as a starting model, Rietveld PXRD full profile structure analyses were performed on the new materials $(TMA)_2MnGe_4Se_{10}$ and $(TMA)_2FeGe_4Se_{10}$. The initially guessed structure refined fairly well in both cases, to yield final R_p values of 8.98% (Mn) and 5.13% (Fe) indicative of a reliable structure determination. A pertinent graphical projection of the Rietveld crystal structures of the $(TMA)_2MnGe_4Se_{10}$ and $(TMA)_2FeGe_4Se_{10}$ frameworks is shown in Fig. 4.

Inspection of the unit-cell dimensions, pertinent bond lengths and angles of the precursors $(TMA)_4Ge_4X_{10}$ and products $(TMA)_2MGe_4X_{10}$, where M = Mn or Fe and X = S or Se,

Table 5 Atomic coordinates [×10^{-4}] and equivalent isotropic displacement parameters [Å^2 × 10^{-3}] for $(TMA)_4Ge_4Se_{10}$

Atom	x	y	z	U(eq)*
Ge(1)	675(1)	675(1)	675(1)	17(1)
Ge(2)	708(1)	5634(1)	1823(1)	16(1)
Se(1)	1324(2)	1324(2)	1324(2)	30(2)
Se(2)	0	0	1381(2)	21(1)
Se(3)	0	5000	1113(1)	17(1)
Se(4)	1368(1)	4926(1)	2508(1)	19(1)
Se(5)	1399(1)	6269(2)	1202(1)	28(1)
N(1)	3372(9)	3372(9)	3372(9)	26(8)
C(1)	2960(12)	2960(12)	2960(12)	47(14)
C(2)	3197(12)	3203(11)	4096(10)	36(7)
N(2)	1508(8)	3392(7)	813(8)	18(4)
C(3)	1664(11)	4123(10)	712(10)	33(5)
C(4)	2007(9)	2968(10)	423(8)	34(5)
C(5)	1611(11)	3257(10)	1568(10)	38(7)
C(6)	826(9)	3223(10)	624(9)	31(5)

* U(iso) is defined as one third of the trace of the orthogonalized U_{ij} tensor.

Table 6 Pertinent crystallographic information for $(TMA)_4Ge_4X_{10}$, where X = S or Se

	Cubic $P\bar{4}3n$	
Parameter	$(TMA)_4Ge_4S_{10}$*	$(TMA)_4Ge_4Se_{10}$
a/Å	19.390(3)	20.028(2)
U/Å^3	7290.1(2)	8033.3(13)
$r(GeX_t)$/Å	2.158(13)	2.253(7)
$r(GeX_b)$/Å	2.244(3)	2.378(2)

* Single-crystal XRD structure determination on the material prepared from the elemental Ge–S precursors.[5] The authors of this reference synthesized the same product from freshly prepared GeS_2.

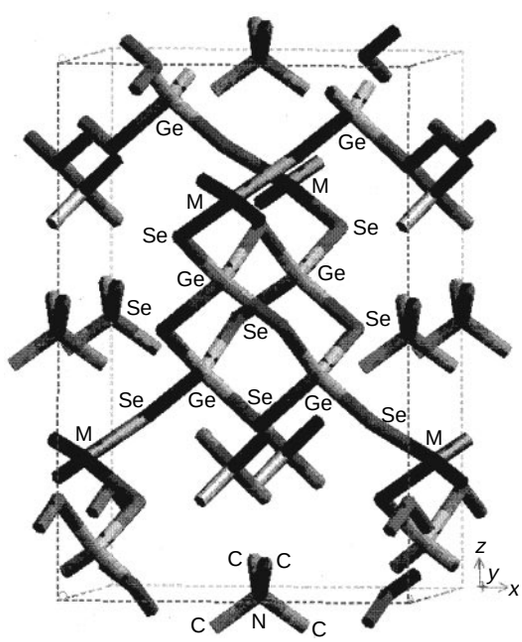

Fig. 4 A CERIUS® molecular graphics representation of $(TMA)_2MGe_4Se_{10}$ showing the adamantanoid $Ge_4X_{10}^{4-}$ and M^{2+} on alternate tetrahedral sites of a zinc-blende lattice. The TMA^+ charge balancing cations occupy the void space of the open framework structure (hydrogen atoms are omitted for clarity)

reveals the expected trends on passing from the smaller S^{-II} and Fe^{II} to the larger Se^{-II} and Mn^{II}, respectively, Table 1. The similarity of the bond lengths and angles in the adamantanoid Ge_4X_{10} cluster in both the modular precursors and the open-framework products indicates that it is behaving as a rigid 'pseudo-tetrahedral' connecting unit. Particularly interesting is

the local co-ordination geometry of the M^{2+} linking site which is a squashed MX_4 tetrahedral (S_4 site symmetry) for all members of the family. The distortion from T_d is most pronounced for $(TMA)_2MnGe_4Se_{10}$ and least for $(TMA)_2FeGe_4S_{10}$, although the angular spread is only $\Delta\alpha = 8.5$ and $\Delta\beta = 3.6°$ for the entire series. This structure-bonding model accounts for the roughly proportional expansion of the unit cell dimensions without any major angular distortions between the building-blocks on passing from the smaller to the larger framework element constituents.

From the X-ray diffraction results one can infer that there are local bond length and angular distortions for the $3d^5$, Mn^{2+}/$3d^6$, Fe^{2+} and $Ge_4X_{10}^{4-}$ modular building-blocks in $(TMA)_2MGe_4X_{10}$ family members. These distortions are away from the regular T_d symmetry sites in the archetype zinc blende-type lattice. They likely arise from the response of the entire system to co-operative TMA^+–framework interactions (*i.e.* TMA^+ template space-filling, charge-balancing and hydrogen-bonding considerations) in order to achieve a structure with the minimum energy configuration.

Acknowledgements

G. A. O. is deeply indebted to the Canada Council for the award of an Isaac Walton Killam Research Fellowship, 1995–1997. The generous financial assistance of the Natural Sciences and Engineering Research Council of Canada (NSERC), the Canadian Space Agency (CSA), and Universal Oil Products (UOP), is deeply appreciated. Dr. S. K. is deeply grateful to NSERC for a graduate scholarship in support of his research. In addition we thank Mr. G. Vovk for synthesizing the $(TMA)_4Ge_4S_{10}$ material discussed in this paper.

References

1 C. N. R. Rao and J. Gopalakrishnan, *New Directions in Solid State Chemistry*, Cambridge University Press, Cambridge, 1986.
2 R. Gunshor and A. V. Nurmikko, *Mater. Res. Bull.*, 1995, **20**, 15.
3 H. Ahari, R. L. Bedard, C. L. Bowes, T. Jiang, A. Lough, G. A. Ozin, S. Petrov and D. Young, *Adv. Mater.*, 1995, **7**, 375.
4 H. Ahari, R. L. Bedard, A. Lough, S. Petrov, G. A. Ozin and D. Young, *Adv. Mater.*, 1995, **7**, 370; H. Ahari, Ö. Dag, R. L. Bedard, S. Petrov and G. A. Ozin, *J. Phys. Chem.*, 1998, **102**, 2356.
5 O. M. Yaghi, Z. Sun, D. A. Richardson and T. L. Groy, *J. Am. Chem. Soc.*, 1994, **116**, 807.
6 O. M. Yaghi, D. A. Richardson, G. Li, C. E. Davis and T. L. Groy, *Mater. Res. Soc. Symp. Proc.*, 1995, **371**, 15.
7 O. Achak, J. Y. Pivan, M. Maunaye, D. Louër and M. Louër, *J. Alloys Comp.*, 1995, **219**, 111.
8 L. Bowes, A. Lough, A. Malek, G. A. Ozin, S. Petrov and D. Young, *Chem. Ber.*, 1996, **129**, 283.
9 C. Larson and R. B. Von Dreele, Los Alamos Laboratory Report No. LA-UR-86-748, 1987.
10 C. K. Johnson, ORTEP, Report ORNL-5138, Oak Ridge National Laboratory, Oak Ridge, TN, 1976.
11 CERIUS$^{2.0®}$, *Simulation Tools User's Reference*, Biosym/Molecular Simulations, San Diego, CA, 1997.
12 G. M. Sheldrick, SHELXA-90, program for absorption correction, University of Göttingen, 1990.
13 G. M. Sheldrick, SHELXTL/PC V5.0, Siemens Analytical X-Ray Instruments, Madison, WI, 1993.
14 S. J. Kirkby, Ph.D. Thesis, *Spectroscopy and Crystallography of Metal Germanium Chalcogenide Openframework Materials and Precursors*, University of Toronto, 1996.

Received 16*th January* 1998; *Paper* 8/00449H